Available online at www.sciencedirect.com

ScienceDirect

Mendeleev Commun., 2019, **29**, 83–85

Mendeleev Communications

Effect of Pb^{2+} ions in solution on the galvanic displacement of lead by platinum

Yurii M. Maksimov,[a] Boris I. Podlovchenko,*[a] Dmitry S. Volkov,[a] Konstantin I. Maslakov[a] and Stanislav A. Evlashin[b]

[a] *Department of Chemistry, M. V. Lomonosov Moscow State University, 119991 Moscow, Russian Federation. Fax: +7 495 939 0171; e-mail: podlov@elch.chem.msu.ru*

[b] *Skolkovo Institute of Science and Technology, 143026 Moscow, Russian Federation. E-mail: s.evlashin@skoltech.ru*

DOI: 10.1016/j.mencom.2019.01.028

The ions Pb^{2+} present in solution during the galvanic displacement of lead by platinum strongly affect the composition, structure, and electrocatalytic properties of Pt^0(Pb) composites.

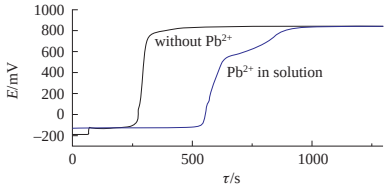

In line with the development of fuel cells, interest in the formic acid electrooxidation reaction (FAOR) does not wane.[1–5] One can substantially increase the activity of platinum in FAOR using two-component Pt–M_1 systems, where M_1 is a cheap non-noble metal.[1,3–8] According to numerous publications, lead is one of the most promising M_1 metals.[1,3–12] Earlier,[4] we found that FAOR-active mixed Pt–Pb catalysts can be synthesized by the galvanic displacement (GD) of Pb by platinum and also studied how this displacement [lead electrolytic deposit (e.d.)] proceeds in the absence of Pb^{2+} ions from solution. It was of interest to carry out the GD of lead by platinum in the presence of Pb^{2+} ions under the conditions described previously[4] and to compare the results with the previous data[4] in order to obtain additional information on the role of lead adatoms (Pb_{ad}) in the formation of a surface layer during the displacement of lead by platinum.

The preparation of e.d. Pb on glassy carbon (GC), the procedure of GD of Pb by Pt, the reagents, and the methods of physicochemical characterization of samples were described previously.[4] A fundamental difference between this work and previous experimental studies[4] is that, in the present study, the displacement of lead by Pt was carried out in a 10^{-2} M $Pb(ClO_4)_2 + 10^{-3}$ M $K_2PtCl_4 +$ + 0.1 M $HClO_4$ solution rather than in 10^{-3} M $K_2PtCl_4 + 0.1$ M $HClO_4$. Henceforth, the deposits formed by GD in the solution containing no Pb^{2+} are designated as Pt^0(Pb)-I and those obtained in the solution with Pb^{2+} are designated as Pt^0(Pb)-II. Samples of composites subjected to potential cycling in the E interval of 0.05–1.45 V are marked by the subscript nc, where n is the number of cycles. Potentials E are related to the reversible hydrogen electrode (RHE) in 0.1 M $HClO_4$ solution at a working temperature of 20 ± 1 °C. The activity of samples was tested with respect to stationary currents of HCOOH electrooxidation in 0.5 M HCCOH + 0.1 M $HClO_4$ solution normalized to cm^2 of the electrochemically active surface area (EASA).[4]

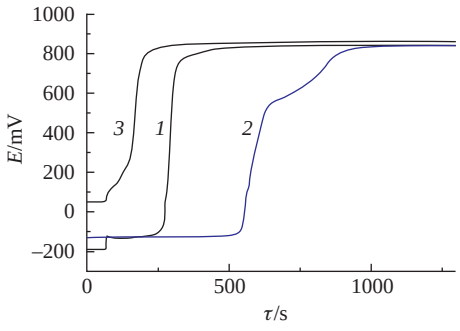

Figure 1 Transients of open-circuit potential upon the introduction of (*1*,*2*) e.d. Pb/GC and (*3*) e.d. Pt/GC into contact with (*1*,*3*) 10^{-3} M $K_2PtCl_4 +$ + 0.1 M $HClO_4$ and (*2*) 10^{-2} M $PbClO_4 + 10^{-3}$ M $K_2PtCl_4 + 0.1$ M $HClO_4$.

Figure 1 shows transients of open-circuit potential (TOCP) observed upon the introduction of e.d. Pb into contact with solutions containing either 10^{-3} M $PtCl_4^{2-}$ (curve *1*) or 10^{-3} M $PtCl_4^{2-} +$ + 10^{-2} M Pb^{2+} (curve *2*) by the background of 0.1 M $HClO_4$. Both types of E *vs.* τ curves demonstrate a characteristic plateau in the potential region approximately in the interval from –150 to –80 mV. This longer plateau corresponds to the transition of a part of Pb atoms to lead ions at the expense of the reduction of $PtCl_4^{2-}$ ions to Pt and also to the partial dissolution of Pb according to the overall reaction $Pb + 2H^+ \rightarrow Pb^{2+} + H_2$.[4]

The reactions that proceed in the region $E < 0$ upon the contact of e.d. Pb with acidic solution of $PtCl_4^{2-}$ can be written as follows:

$$Pb + PtCl_4^{2-} \rightarrow Pt^0 + Pb^{2+} + 4Cl^-, \quad (1)$$

$$Pt^0 + 2H^+ + 2e^- \rightarrow Pt^0\,(H_2), \quad (2)$$

$$Pb - 2e^- \rightarrow Pb^{2+}. \quad (3)$$

The exchange current of the reaction $2H^+ + 2e^- \leftrightarrow H_2$ on platinum is higher by five or six orders of magnitude than that on lead.[13]

The ICP-AES analysis of the composites (Table 1) showed that, at the formation of Pt^0(Pb)-I, about 50% of Pb dissolves as a result of discharge of H^+, in contrast to Pt^0(Pb)-II, which is formed by reaction (1) with only ~15% due to the hydrogen reaction. This difference can be explained by the fact that, when Pb^{2+} is present in solution, the rate of formation of Pb_{ad} sharply increases at $E < 0$. This results in the inhibition of both reaction (2) and the overall process of Pb dissolution and can explain the much longer arrest in the region $E < 0$ when Pb^{2+} is present in solution. The total mass of the deposit formed in the presence of Pb^{2+} is larger

Table 1 Surface and volume composition of Pt^0(Pb)–I and Pt^0(Pb)–II composites.

Sample	Method	Pt		Pb	
		at%	μg	at%	μg
Pt^0(Pb)-II	ICP-AES[a]	82.6	170	17.4	38.0
	EDX[b]	86.0		14.0	
	XPS	77.2		22.8	
Pt^0(Pb)-I	ICP-AES[a]	62.0	85	38.0	52.5
	EDX	65.0		35.0	
	XPS	87.5		12.5	

[a] Confidence interval, ±10%. [b] Average value for 7 points.

than the mass of the Pt^0(Pb)-II deposit; moreover, the fraction of Pt in the bulk of this deposit is larger (the mass of initial Pb deposit was 250 ± 10 μg cm^{-2}).[4]

Yet another distinction of TOCP recorded in the presence of Pb^{2+} in solution (see Figure 1, curve *2*) is the well-pronounced arrest near ~550–800 mV. This may be associated with the earlier inhibition of reaction (1) because of the higher surface coverage by Pb_{ad} when Pb^{2+} is present in solution in the concentration much higher than that provided by displacement of Pb (< 3×10^{-5} M). It cannot also be ruled out that the presence of Pb^{2+} in considerable amounts favors the formation of mixed deposits $PtPbO_x$.[5] The stationary potentials for Pt^0(Pb)-I and Pt^0(Pb)-II are almost equal and close to E_{st} established on e.d. Pt in $PtCl_4^{2-}$ solution (see Figure 1, curve *3*). This allowed us to conclude that E_{st} for Pt^0(Pb) composites is determined by reactions on Pt^0.[4]

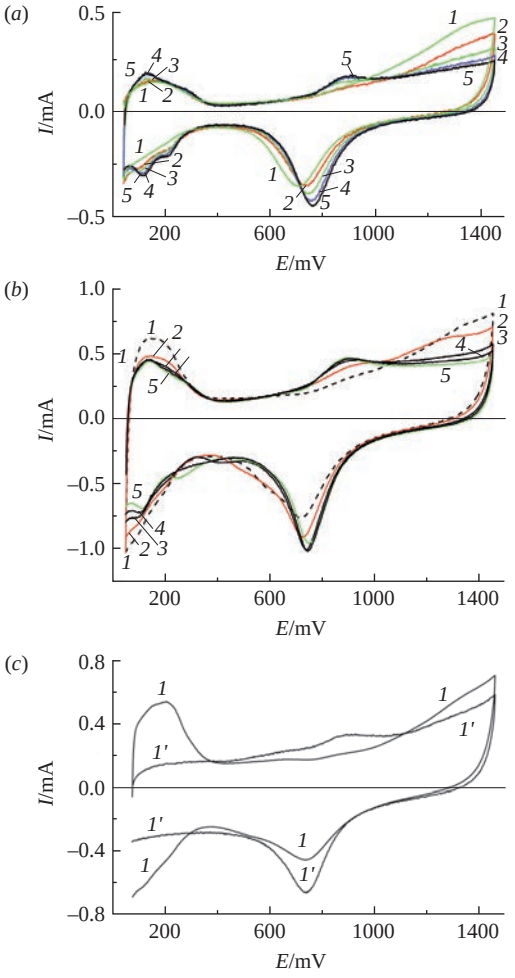

Figure 2 CVA in 0.1 M $HClO_4$ for (*a*) Pt^0(Pb)-I and (*b*, *c*) Pt^0(Pb)-II. Cycle number: (*1*) 1, (*2*) 2, (*3*) 5, (*4*) 10, and (*5*) 20. Curve *1′* in Figure 2(*c*), 1st cycle in 10^{-2} M $PbClO_4$ + 0.1 M $HClO_4$ solution.

The overall XPS spectrum of Pt^0(Pb)–II is similar to that of Pt^0(Pb)-I.[4] The Pt and Pb contents in the surface layer estimated based on the XPS data (see Table 1) show that lead is present in substantial amounts in both samples, but its content in Pt^0(Pb)-II is double that in Pt^0(Pb)-I. The incomplete displacement of Pb from the surface layer by platinum is associated with the fact that a part of Pb_{ad} on Pt desorbs at $E > E_{st}$.[4] Insofar as the surface coverage with Pb_{ad} increases with the Pb^{2+} concentration in solution,[14] it should be expected that the larger amount of lead will be incorporated into the surface layer, which is confirmed experimentally. The XPS spectra of Pt^0(Pb) point to the presence of lead in both its metallic and oxidized forms.

The ionization currents of hydrogen adsorbed on Pt^0(Pb)-II [Figure 2(*b*)] are higher than those on Pt^0(Pb)-I [Figure 2(*a*)], which is probably associated with the high amount of deposited Pt (see Table 1). For EASA assessed from the hydrogen adsorption, the specific values are 16 m^2 g^{-1} for Pt^0(Pb)-I and 11 m^2 g^{-1} for Pt^0(Pb)-II, which are close to the specific surface of e.d. Pt on platinum. In the anodic branch of the first CVA at potentials of oxygen adsorption, the lead ionization currents are observed, which point to the absence of strong Pt shells. However, at the further potential cycling after five or six cycles, the differences in CVA become insignificant and the latter acquire the shape typical of e.d. Pt on GC.[4] This fact points to the formation of a sufficiently strong Pt shell. This is also confirmed by the XPS analysis of samples subjected to 20-fold cycling; the lead contents of surface layers were 7.5 at% for Pt^0(Pb)-I_{20c} and 3.5 at% for Pt^0(Pb)-II_{20c} (Pb at% + Pt at% = 100%). Note that the depth of XPS analysis is 3–4 nm (more than 10 monolayers of Pt); *i.e.*, the first atomic layer may contain a much lower amount of Pb.

According to Figure 2(*b*), for the Pt^0(Pb)-II deposit, the hydrogen sorption considerably decreases with the number of cycles, whereas it changes insignificantly for Pt^0(Pb)-I [Figure 2(*a*)]. However, this difference cannot be considered as fundamental because the variation in the amount of adsorbed hydrogen (Q_H) with the number of cycles was poorly reproducible. The main reason for this may be the action of two competitive factors: the decrease in the amount of lead in the surface layer should favor the increase in Q_H, whereas the restructuring of the deposit with the crystal growth should lead to a decrease in Q_H. It is interesting that the adsorption of hydrogen on Pt^0(Pb) composites is suppressed almost completely when Pb^{2+} cations in the concentration sufficient for the formation of the Pb_{ad} monolayer are added to the background solution[15] [Figure 2(*c*)]. Such an effect was observed at the formation of the Pb_{ad} monolayer on smooth polycrystalline Pt and e.d. Pt.[4,15] This allows us to assume that platinum can conglomerate to form sufficiently large islets at least in the upper atomic layer of Pt^0(Pb).

The specific stationary currents of FAOR on freshly formed Pt^0(Pb)-II catalyst (Figure 3, curve *1*) are much higher (~20-fold)

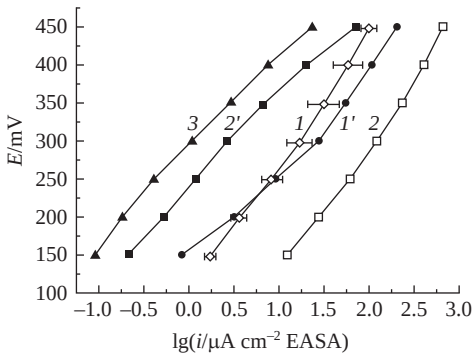

Figure 3 Stationary polarization curves of FAOR on (*1*) Pt^0(Pb)-II, (*1′*) Pt^0(Pb)-II_{20c}, (*2*) Pt^0(Pb)-I, (*2′*) Pt^0(Pb)-I_{20c}, and (*3*) e.d. Pt; 0.5 M HCOOH + + 0.1 M $HClO_4$.

Table 2 Surface layer composition of Pt–Pb composites and their specific activity in FAOR (at 200 mV).

Sample	Composite	A_{Pb} (at%)	$\lg(i_{200}/\mu A\ cm^{-2})$
1	$Pt^0(Pb)$-I	12.5	1.40
2	$Pt^0(Pb)_{20c}$-I	7.5	–0.25
3	$Pt^0(Pb)$-II	23.0	0.60
4	$Pt^0(Pb)_{20c}$-II	3.5	0.50
5	e.d. PtPb[5]	76.0	2.20
6	e.d. $PtPb_{20c}$[5]	2.6	0.30
7	e.d. Pt	–	–0.75

than the analogous currents on e.d. Pt (curve *3*); however, on $Pt^0(Pb)$-II the effect of FAOR promotion is far weaker than on $Pt^0(Pb)$-I (curve *2*). Thus, the presence or absence of Pb^{2+} in solution at GD has a substantial effect on the electrocatalytic activity of the $Pt^0(Pb)$ binary catalysts. This effect could be associated with the larger amount of Pb in the surface layer of $Pt^0(Pb)$-II as compared with $Pt^0(Pb)$-I (see Table 1). This is why it was of interest to correlate the surface composition of Pt–Pb catalysts (XPS data) with their activity in FAOR, based on the corresponding data for $Pt^0(Pb)$-I[4] and $Pt^0(Pb)$-II (this study), and e.d. PtPb.[5]

Table 2 presents such a comparison for E = 200 mV. It is evident that the presence of lead in the surface layer activates Pt in FAOR, but no correlation is observed between the Pb content (A_{Pb}) and the activation level. Thus, samples 1 and 2 contain close amounts of Pb in the surface layer, however their activities differ by a factor of ~40; the highest activity is exhibited by samples 1 and 5 containing 12.5 and 76 at% Pb, respectively. The above suggests that the promotion of Pt by lead additions depends on a complex of factors such as changes in the electronic state of Pt atoms (electronic factor), a decrease in the contribution of areas suitable for n-site adsorption of strongly chemisorbed species, the effect of structure defects, and the bifunctional catalysis.[3–12] To date it is impossible to distinguish the contributions of each of these factors.

The $Pt^0(Pb)$-II composite differs substantially from the $Pt^0(Pb)$-I composite not only in the polarization characteristics of FAOR but also in the stability of these characteristics. The activity of $Pt^0(Pb)$-II after 20-fold potential cycling does not change significantly (Figure 3, curve *1′*), whereas the activity of $Pt^0(Pb)$-I decreases considerably (curve *2′*).

It was assumed[4] that the bifunctional catalysis[16] associated with the generation of active oxygen forms on Pb inclusions is highly improbable at least in the potential region of hydrogen adsorption (lower than ~350 mV, according to Figure 2). At the same time, in the previous study,[4] we ignored the fact that, at these potentials, lead atoms may move from the catalyst bulk to the surface to form lead adatoms on Pt clusters. In turn, the presence of the adatoms should be accompanied by the appearance of Pb^{2+} ions in the near-surface solution layer. This makes possible the overall reaction $Pb^{2+} + HCOOH \rightarrow Pb_{ad} + 2H^+ + CO_2$, *i.e.*, the pair Pb_{ad}/Pb^{2+} can provide the mediator catalysis of HCOOH oxidation. To elucidate whether FAOR can proceed even if partially by the proposed route, we performed the following experiment. Two samples of the original composite $Pt^0(Pb)$-II were held at 300 mV for 6 h: one in 0.1 M $HClO_4$ solution and the other in 0.5 M HCOOH + 0.1 M $HClO_4$ (both solutions were deaerated). In the former case, 67 μg of lead passed to solution and, in the latter case, 34 μg, *i.e.*, only a half. This counts in favor of interaction between Pb^{2+} ions and HCOOH molecules in the near-surface layer. The catalysis of mediator type can most probably occur on samples with the higher Pb content in the surface layer. Note that the effect of different factors on the activity of Pt–M_1 composites depends on the length and type of the Pt/M_1 interface.[4,5,17,18]

This work was supported by the Russian Foundation for Basic Research (project no. 17-08-01414A) and, in part, by the M. V. Lomonosov Moscow State University Program of Development.

References

1 K. Jiang, H.-X. Zhang, S. Zou and W.-B. Cai, *Phys. Chem. Chem. Phys.*, 2014, **16**, 20360.
2 S. Ha, Z. Dunbar and R. I. Masel, *J. Power Sources*, 2006, **158**, 129.
3 R. R. Adžić, A. V. Tripković and N. M. Marković, *J. Electroanal. Chem.*, 1983, **150**, 79.
4 B. I. Podlovchenko and Yu. M. Maksimov, *J. Electroanal. Chem.*, 2017, **801**, 319.
5 Yu. M. Maksimov, B. I. Podlovchenko, E. A. Vyrko, S. A. Evlashin and D. S. Volkov, *Mendeleev Commun.*, 2018, **28**, 178.
6 M. Shibata and S. Motoo, *J. Electroanal. Chem.*, 1985, **188**, 111.
7 E. Casado-Rivera, D. J. Volpe, L. Alden, C. Lind, C. Downie, T. Vázquez-Alvarez, A. C. D. Angelo, F. J. DiSalvo and H. D. Abruña, *J. Am. Chem. Soc.*, 2004, **126**, 4043.
8 B. I. Podlovchenko, Yu. M. Maksimov, S. A. Evlashin, T. D. Gladysheva, K. I. Maslakov and V. A. Krivchenko, *J. Electroanal. Chem.*, 2015, **743**, 93.
9 Y. Huang, S. Zheng, X. Lin, L. Su and Y. Guo, *Electrochim. Acta*, 2012, **63**, 346.
10 S. Papadimitriou, A. Tegou, E. Pavlidou, G. Kokkinidis and S. Sotiropoulos, *Electrochim. Acta*, 2007, **52**, 6254.
11 G. Saravanan, K. Nanba, G. Kobayashi and F. Matsumoto, *Electrochim. Acta*, 2013, **99**, 15.
12 J. V. Perales-Rondón, J. Solla-Gullón, E. Herrero and C. M. Sánchez-Sánchez, *Appl. Catal., B*, 2017, **201**, 48.
13 K. J. Vetter, *Elektrochemische Kinetik*, Springer-Verlag, Berlin, 1961.
14 D. M. Kolb, in *Advances in Electrochemistry and Electrochemical Engineering*, eds. H. Gerischer and C. W. Tobias, Wiley, New York, 1978, vol. 11, pp. 125–271.
15 N. Dimitrov, *Electrochim. Acta*, 2016, **209**, 599.
16 M. Watanabe and S. Motoo, *J. Electroanal. Chem.*, 1975, **60**, 267.
17 V. V. Kusnetsov, B. I. Podlovchenko, R. I. Shakurov, K. V. Kavyrshina and S. E. Lyahenko, *Int. J. Hydrogen Energy*, 2014, **39**, 829.
18 Yu. M. Maksimov, B. I. Podlovchenko, E. M. Gallyamov, S. A. Dagesyan, V. V. Sen and S. A. Evlashin, *Mendeleev Commun.*, 2017, **27**, 382.

Received: 23rd April 2018; Com. 18/5578